โครงการ
การเรียนการสอนเพื่อเสริมประสบการณ์

ชื่อโครงการ การสังเคราะห์และทดสอบประสิทธิภาพการเป็นตัวเร่งปฏิกิริยาของเตตระอะมิโน

พทาโลไซยานีนสำหรับปฏิกิริยารีดักชันของคาร์บอนไดออกไซด์

Synthesis and investigation of tetraaminophthalocyanines
for electrocatalytic reduction reaction of carbon dioxide

ชื่อนิสิต นายธีทัต ตรีสุคนธ์   **เลขประจำตัว** 5933053023

ภาควิชา เคมี

ปีการศึกษา 2562

คณะวิทยาศาสตร์ จุฬาลงกรณ์มหาวิทยาลัย

การสังเคราะห์และทดสอบประสิทธิภาพการเป็นตัวเร่งปฏิกิริยาของเตตระอะมิโน
พทาโลไซยานีนสำหรับปฏิกิริยารีดักชันของคาร์บอนไดออกไซด์

Synthesis and investigation of tetraaminophthalocyanines
for electrocatalytic reduction reaction of carbon dioxide

โดย
นายธีทัต ตรีสุคนธ์

รายงานนี้เป็นส่วนหนึ่งของการศึกษาตามหลักสูตร
ปริญญาวิทยาศาสตรบัณฑิต
ภาควิชาเคมี คณะวิทยาศาสตร์
จุฬาลงกรณ์มหาวิทยาลัย
ปีการศึกษา 2562

Synthesis and investigation of tetraaminophthalocyanines
for electrocatalytic reduction reaction of carbon dioxide

Mr. Teedhat   Trisukhon

In Partial Fulfilment for the Degree of Bachelor of Science

Department of Chemistry, Faculty of Science

Chulalongkorn University

Academic Year 2019

Project Title: Synthesis and investigation of tetraaminophthalocyanines for electrocatalytic reduction reaction of carbon dioxide

Student name: Mr. Teedhat Trisukhon

Accepted by Department of Chemistry, Faculty of Science, Chulalongkorn University in Partial Fulfillment of the Requirement for the Bachelor of Science.

PROJECT COMMITTEE

1. Associate Professor Dr. Buncha Pulpoka   Chair Committee
2. Assistant Professor Dr. Charoenkwan Kraiya   Committee
3. Professor Dr. Patchanita Thamyongkit   Project Advisor

This report has been approved by the Head of the Department of Chemistry.

....
(Professor Patchanita Thamyongkit, Dr.rer.nat.)
Project Advisor

....
(Associate Professor Vudhichai Parasuk, Ph.D.)
Head of Department of Chemistry

............10...../....06...../ 2020

ชื่อโครงการ   การสังเคราะห์และทดสอบประสิทธิภาพการเป็นตัวเร่งปฏิกิริยาของเตตระอะมิโน
                    พทาโลไซยานีนสำหรับปฏิกิริยารีดักชันของคาร์บอนไดออกไซด์
ชื่อนิสิตในโครงการ   นายธีทัต ตรีสุคนธ์   เลขประจำตัว 5933053023
ชื่ออาจารย์ที่ปรึกษา   ศาสตราจารย์ ดร. พัชณิตา ธรรมยงค์กิจ
ภาควิชาเคมี คณะวิทยาศาสตร์ จุฬาลงกรณ์มหาวิทยาลัย ปีการศึกษา 2562

บทคัดย่อ

งานวิจัยนี้ได้สังเคราะห์และศึกษาความสามารถในการเร่งปฏิกิริยารีดักชันเชิงเคมีไฟฟ้าของคาร์บอนได-ออกไซด์แบบเอกพันธ์ของสารประกอบโคบอลต์(II)-, นิกเกิล(II)- และ คอปเปอร์(II)- พทาโลไซ-ยานีนที่ถูกปรับปรุงโครงสร้างด้วยหมู่อะมิโน การเพิ่มขึ้นของกระแสไฟฟ้ารีดักชันภายใต้ภาวะอิ่มตัวด้วยคาร์บอนไดออกไซด์ที่ศึกษาด้วยวิธีไซคลิกโวลแทมเมตทรีแสดงถึงการมีส่วนร่วมของสารเชิงซ้อนทุกชนิดในกระบวนการรีดักชันเชิงเคมีไฟฟ้าของคาร์บอนไดออกไซด์ เมื่อทำการให้ศักย์ไฟฟ้า -1.6 โวลต์เทียบกับขั้วไฟฟ้าอ้างอิงซิลเวอร์/ซิลเวอร์คลอไรด์ชนิดควอซ เป็นระยะเวลา 2 ชั่วโมงด้วยเทคนิคโครโนแอมเปอโรแมทรี และวิเคราะห์ผลิตภัณฑ์ด้วยเทคนิคแก๊สโครมาโตกราฟ พบว่าโคบอลต์(II)-, นิกเกิล(II)- และ คอปเปอร์(II)- พทาโลไซยานีนให้แก๊สไฮโดรเจนเป็นผลิตภัณฑ์โดยมีประสิทธิภาพฟาราเดย์เท่ากับ 32%, 35% และ 39% ตามลำดับ แต่มีเพียงโคบอลต์(II)-, นิกเกิล(II)- พทาโลไซยานีนเท่านั้นที่ให้แก๊สคาร์บอนมอนอกไซด์เป็นผลิตภัณฑ์ด้วยประสิทธิภาพฟาราเดย์เท่ากับ 1.6%, 0.2% จากผลการทดลองสรุปได้ว่าระบบปฏิกิริยาไฟฟ้าเคมีโดยมีโคบอลต์(II)-พทาโลไซยานีนเป็นตัวเร่งปฏิกิริยามีแนวโน้มในการผลิตแก๊สคาร์บอนมอนอกไซด์สูงที่สุด ในขณะที่ระบบปฏิกิริยาไฟฟ้าเคมีโดยคอปเปอร์(II)-พทาโลไซยานีนเป็นตัวเร่งปฏิกิริยาเหมาะสำหรับการสังเคราะห์แก๊สไฮโดรเจน

คำสำคัญ: เมทาโลพทาโลไซยานีน; ตัวเร่งปฏิกิริยาเชิงเคมีไฟฟ้า; ตัวเร่งปฏิกิริยาเอกพันธ์; ปฏิกิริยารีดักชันเชิงเคมีไฟฟ้าของคาร์บอนไดออกไซด์

Project Title   Synthesis and investigation of tetraminophthalocyanines
        for electrocatalytic reduction reaction of carbon dioxide
Student Name Mr. Teedhat Trisukhon   Student ID 5933053023
Advisor Name Professor Patchanita Thamyongkit, Dr.rer.nat.
Department of Chemistry, Faculty of Science, Chulalongkorn University,
Academic Year 2019

Abstract

In this work, synthesis and investigation on homogeneous catalytic activities for electrochemical reduction (ECR) of carbon dioxide (CO_2) of amino-functionalized Co(II)-, Ni(II)-, and Cu(II)- phthalocyanines were described. Current enhancement under CO_2-saturated condition observed by cyclic voltammetry indicated involvement of all complexes in the ECR of CO_2. Chronoamperometry applying potential of -1.6 V vs. Ag/AgCl QRE for 2 h, followed by product analysis by gas chromatography showed that amino-functionalized Co(II)-, Ni(II)-, and Cu(II)-phthalocyanines yielded hydrogen gas (H_2) with %Faradaic efficiency (%FE) of 32%, 35% and 39%, respectively. However, only amino-functionalized Co(II)- and Ni(II)- phthalocyanines yielded carbon monoxide (CO) with %FE of 1.6% and 0.2%, respectively. The results indicated that it is promising to further develop Co(II)-phthalocyanine-based electrocatalytic system for the production of CO while the Cu(II)-phthalocyanine-based one seems to be suitable for H_2 evolution.

Keywords: Metallophthalocyanine; Electrocatalyst; Homogenous catalyst;
     Electrochemical reduction of carbon dioxide

ACKNOWLEDGEMENTS

CONTENTS

LIST OF FIGURES

LIST OF SCHEMES

LIST OF TABLES

Chapter I

Introduction and literature reviews

1.1 Introduction

Due to rapid global industry and population growth, demand for fossil fuel consumption is getting increased[1]. Consequently, emission of carbon dioxide (CO_2) to atmosphere from combustion of the fossil fuel tends to increase, causing an environmental problem so-called "Global warming".[2,3] Using renewable energy is an alternative practical way to reduce amount of the CO_2 emission. However, renewable energy along with the fossil fuel has yet to meet energy demands.[4] As a result, CO_2 capture and storage (CCS) technology has been considered as an approach for reducing the amount of CO_2 emission by using absorbents or adsorbents to absorb or adsorb CO_2, respectively, through physical and chemical processes.[5] Furthermore, the economic value of collected CO_2 can be increased by coupling the CO_2 capturing methods with suitable CO_2 conversion technologies. Electrochemical reduction (ECR) of CO_2 is one of the most interesting CO_2 conversion techniques as it can be performed under ambient conditions in aqueous media and is compatible with utilization of other renewable energy sources.[6] This method is achieved by electrochemically reducing CO_2 into useful chemicals, such as carbon monoxide (CO), formic acid (HCOOH), methanol (CH_3OH), methane (CH_4), etc.[7] However, since CO_2 is a very stable molecule and requires high overpotential to get reduced to $CO_2^{\cdot-}$ intermediate in the aqueous media,[8] electrocatalysts are very necessary in the ECR of CO_2. Lately, metals,[9] metal oxides,[10] metal chalcogenides,[11] heteroatom-doped carbons (e.g. nitrogen-doped carbon nanotubes and carbon nanofibers),[12, 13] and metal organic complexes[14] have been reported as the electrocatalysts for the ECR of CO_2. Among these materials, metallophthalocyanines (MPc) are of a great interest because of their remarkable advantages in terms of accessibility, chemical stability and structural tunability.[15] Electrocatalytic activities of the MPc for the ECR of CO_2 can be improved by introducing central metals, such as Cu(II),[16] Co(II),[17] Fe(II)[18] and Ni(II),[19] and modifying different functional groups on peripheral positions of phthalocyanine macrocycles, such as an amino group to capture the CO_2 molecules.[20] In this work, we are interested in synthesis and investigation of catalytic performance towards the ECR of CO_2 of MPc derivatives containing the peripheral amino groups and non-precious-metal centers, *i.e.* Co(II), Ni(II), and Cu(II), structures of which are

shown in **Figure 1-1**. The overview presented in this work on the effect of the central metals on the electrochemical behavior and electrocatalytic activities of these amino-functionalized MPc derivatives for the ECR of CO_2 will become a helpful guideline for further development of several oligopyrrole-based electrocatalytic systems.
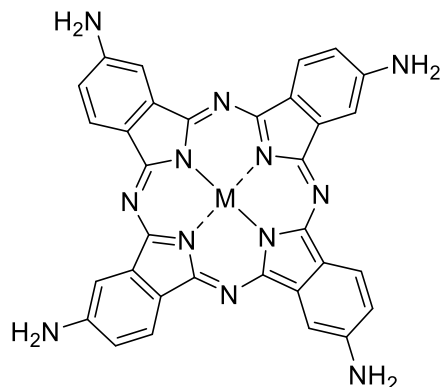
Figure 1-1: Structures of the target molecules
CoTAPc ; M = Co
NiTAPc ; M = Ni
CuTAPc ; M = Cu

1.1.1 Objectives of this research

Synthesis and investigation of the electrochemical properties, as well as the catalytic activities towards the ECR of CO_2 of the amino-functionalized Co(II)-, Ni(II)-, and Cu(II)-Pc derivatives.

1.1.2 Scopes of this research

The target amino-functionalized MPc derivatives contain Co(II), Ni(II) or Cu(II) as a metal center. They were characterized by spectroscopic techniques, including mass spectrometry (MS) and UV-visible absorption spectrophotometry. The electrochemical properties of solutions of the target compounds were investigated by cyclic voltammetry (CV) and their electrocatalytic performance for the homogeneous ECR of CO_2 was studied by CV and chronoamperometry (CA). Both electrochemical techniques were investigated under CO_2 saturated condition, compared with the study under N_2 saturation at ambient temperature and pressure.

1.2 Theory and Literature Reviews

1.2.1 Phthalocyanine (Pc)

Pc is a large, aromatic, macrocyclic, organic compound with the chemical formula of $(C_8H_4N_2)_4H_2$, structure of which is shown in **Figure 1-2**.[21] Pc consists of four isoindole units linked by nitrogen atoms with a ring system consisting of 18 π-electrons and has a two-dimensional geometry. An additional π-orbital conjugation is formed by four benzo-fused rings. Therefore, Pc derivatives are generally thermally and chemically stable: they withstand up to 500 °C under high vacuum and tolerate action of non-oxidative acids or bases without decomposition.[22] Complexation to form MPc can easily be achieved by direct metalation between Pc and several kinds of metal salts. Even though there might be an unfavorable metal ion oxidation states formed in MPc, they would be stabilized due to an electron donor from the Pc ring to finally obtain highly stable MPc.[23]
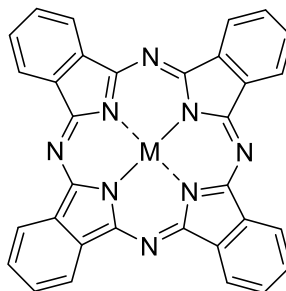
Figure 1-2: A general structure of MPc (for Pc, M is H,H)

Absorption spectra of Pc and MPc as shown in **Figure 1-3**(a) compose of two main absorption bands.[24] The first is a Q-band that is associated to π–π* doubly degenerated transition, *i.e.* a_{1u} to e_g. In a metal-free system, its lower symmetry destroys degeneracy of molecular orbitals and the Q-band is split into two components. The second band is a B-band, appearing as a broad band located at a near ultraviolet region, is due to π–π*transitions from low-energy occupied orbitals to the e_g orbital. According to the chemical and photophysical properties, the Pc and MPc derivatives were used in many applications, such as energy storage,[25] photodynamic cancer therapy,[26] molecular semiconductors,[27] photovoltaic devices,[28] fuel cells[29] and sensors.[30]
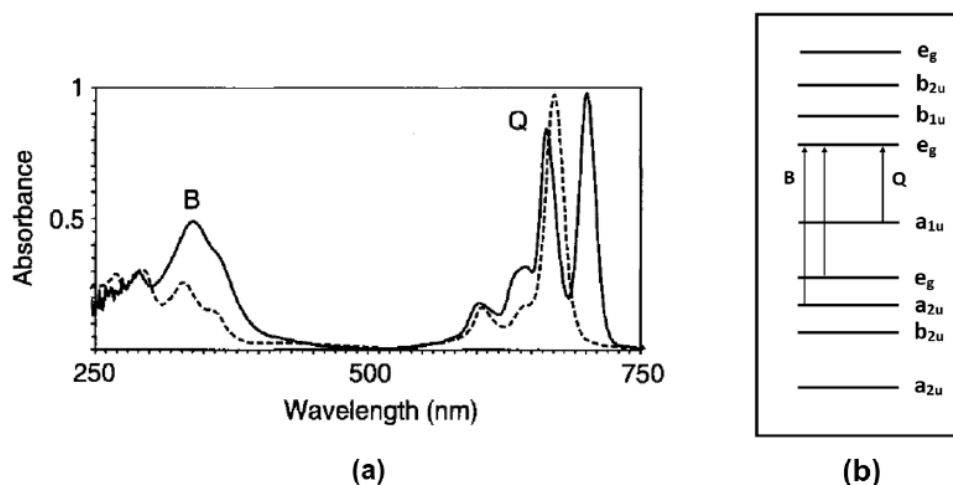
Figure 1-3: (a) UV-vis spectra of Pc (solid line) and MPc (dashed line), and (b) energy levels and transitions for Q and B bands of MPc as reported by John Mack and Martin Stillman[24]

1.2.1.1 Synthesis of phthalocyanine

The Pc derivatives can be synthesized by many routes, some of which are described below.

In 2015, Dhavala and coworkers[31] synthesized Cu(II)phthalocyanine (**CuPc**) in 44% yield from phthalic anhydride in the presence of urea, CuCl and ammonium heptamolybdate under neat condition at 320 ℃ for 5 min as shown in **Scheme 1-1.**
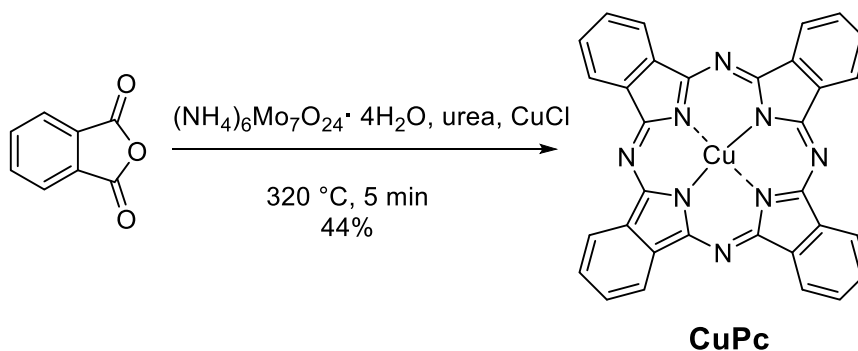
Scheme 1-1: Synthesis of **CuPc** as described by Dhavala *et al.*[31]

In 2017, Mohammed and Kareem[32] synthesized (2,9,16,23-tetranitrophthalocyanato)zinc(II) **(ZnTNPc)** in 57% yield by mixing 4-nitrophthalonitrile and $ZnCl_2$ in dimethylaminoethanol (DMAE) under nitrogen atmosphere and stirred at 185 ˚C for 1 h as shown in **Scheme 1-2**.
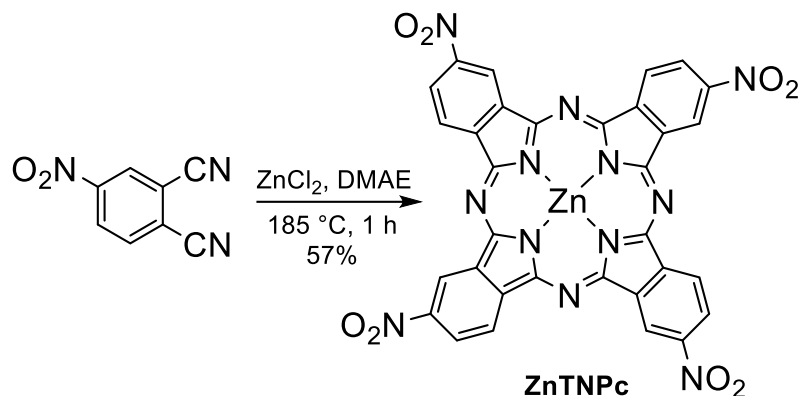
Scheme 1-2: Synthesis of **ZnTNPc** as reported by Mohammed and Kareem[32]

In 2009, Sakamoto and Okumura[33] synthesized (2,9,16,23-tetrasulfonic acid phthalocyanato)copper(II) **(CuTSPc)** from 4-sulfophthalic acid, CuCl, urea and 1,8 diazabicyclo-[5,4,0]undec-7-ene (DBU) at 210 ºC for 180 min as shown in **Scheme 1-3**.
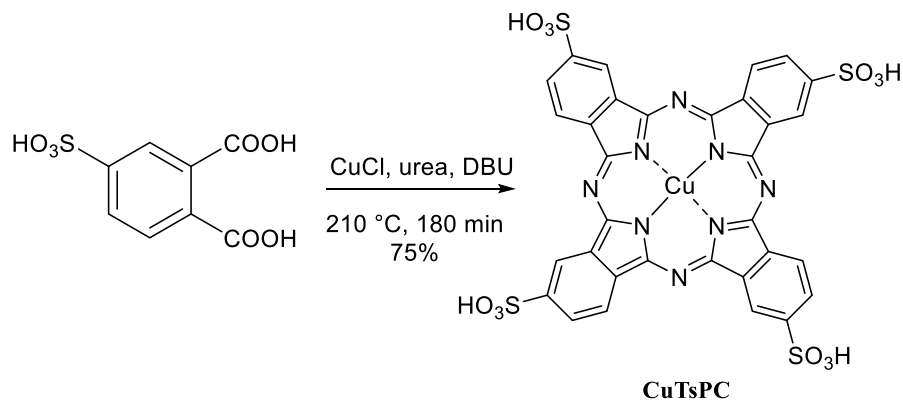
Scheme 1-3: Synthesis of **CuTSPc** as studied by Sakamoto and Okmura[33]

1.2.2 Electrochemical reduction of CO_2

The ECR of CO_2 is an approach to convert CO_2 to fuels and industrial chemicals, for example hydrocarbons and alcohols,[34] by applying electrical potential into an electrolyte solution saturated with CO_2. The electrochemical method has several advantages: (i) the process can be performed at room temperature and under ambient pressure, which is a mild condition; (ii) this method is highly selective and economically friendly; and (iii) electrochemical systems generally have compact designs.[35] A reduction process of the thermodynamically stable CO_2 to unstable $CO_2^{\bullet-}$ requires high potential, *i.e.* up to -1.90 V vs. normal hydrogen electrode (NHE),[36] to drive the reaction. On the other hand, proton-assisted electron transfer processes are more favorable with a lower potential in the range of -0.24 V to -0.61 V vs. NHE.[37] The calculated standard potentials (E^o) to produce various products from the ECR of CO_2 at pH 7 vs. NHE at 25 ºC under 1 atm gas pressure are summarized in Equations 1–6.[38] However, at the similar potential, hydrogen evolution is a competitive process for the ECR of CO_2 on a cathode side. Thereby, the electrocatalyst for the ECR of CO_2 is required to efficiently generate reduction products and provides a feasible way to overcome overpotential.

$$CO_2 + e^- \longrightarrow CO_2^{\bullet-} \qquad E^o = -1.90 \text{ V} \quad (1)$$
$$CO_2 + 2H^+ + 2e^- \longrightarrow HCO_2H \qquad E^o = -0.61 \text{ V} \quad (2)$$
$$CO_2 + 2H^+ + 2e^- \longrightarrow CO + H_2O \qquad E^o = -0.53 \text{ V} \quad (3)$$
$$CO_2 + 4H^+ + 4e^- \longrightarrow HCHO + H_2O \qquad E^o = -0.48 \text{ V} \quad (4)$$
$$CO_2 + 6H^+ + 6e^- \longrightarrow CH_3OH + H_2O \qquad E^o = -0.38 \text{ V} \quad (5)$$
$$CO_2 + 8H^+ + 8e^- \longrightarrow CH_4 + 2H_2O \qquad E^o = -0.24 \text{ V} \quad (6)$$
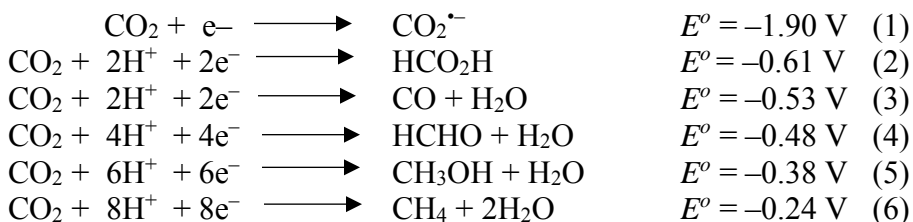
The electrocatalysts can be divided into two types, *i.e.* homogeneous and heterogeneous catalysts. An advantage of the homogeneous catalysts is that the catalysts are molecularly dispersed within the solution. Hence, the reaction mixture allows a very high degree of interaction between catalyst and reactant molecules. However, unlike the heterogeneous catalysts, the homogeneous catalysts are often irrecoverable after the reaction has completed. Furthermore, homogeneous systems often suffer from some drawbacks, such as stability of the catalysts and complex post-separation. Therefore, major efforts have been made to develop heterogeneous electrocatalysts by several approaches, *e.g.* the development of organic frameworks and the use of highly conjugated carbon-based materials.[39]

1.2.3 Electrochemical analysis

1.2.3.1 Cyclic voltammetry (CV)

The CV is a commonly used electrochemical technique to investigate the reduction and oxidation processes of electroactive species. It is also an appropriate technique to study electron transfer-initiated chemical reactions, including catalysis[40] , owing to several advantages; *e.g.* non-destructive nature, versatility and informative details that can be relatively quickly analyzed.[41] In a homogeneous study, the required CV setup consists of a potentiostat connected with three electrodes: working (WE), reference (RE) and counter (CE) electrodes, submerged in an electrolyte sample solution as shown in **Figure 1–4**[42]
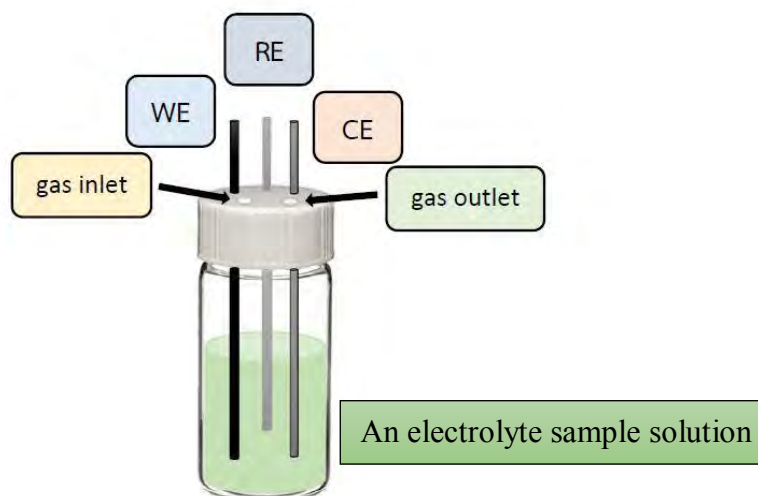
Figure 1-4: A three-electrode one-compartment setup

A CV measurement gives a linearity of potential scanning with a triangular waveform through a potential range and reversing the direction of the sweep in a cyclic wave corresponding to time, as shown in **Figure 1−5a**, to the WE in the stationary electrolyte solution and then measuring the current. The applied potential is controlled relative to the RE, such as a saturated calomel electrode (SCE) or a Silver/Silver Chloride Reference Electrode (Ag/AgCl). A plot between the recorded current as a vertical axis and the applied potential as a horizontal axis is called a cyclic voltammogram, showing a current enhancement and either anodic and/or cathodic peaks where the electrochemical oxidation and/or reduction take place, respectively, as shown in **Figure 1−5b**. In the voltammogram, where a forward scan produces an anodic current for any

analytes that can be oxidized through the range of the scanned potential, the reverse scan gives a cathodic current for the product of the forward scan being reduced. Therefore, there are oxidation and reduction peaks observed for a reversible reaction. Significant parameters in the cyclic voltammogram are a cathodic peak potential (E_{pc}), an anodic peak potential (E_{pa}), a cathodic peak current (I_{pc}) and an anodic peak current (I_{pa}), describing electrochemical behavior of the analyte.[43]
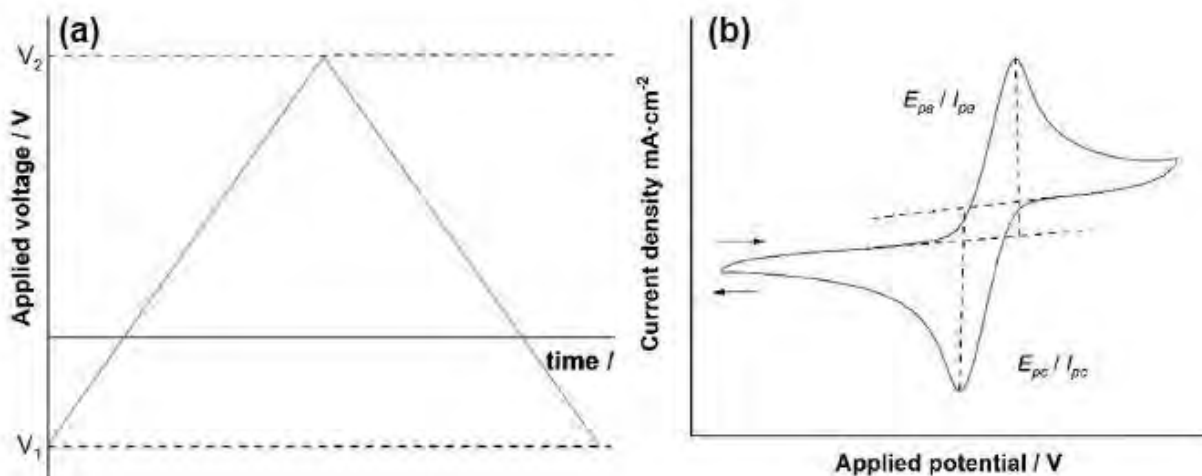
Figure 1-5: (a) A triangular waveform signal and (b) a cyclic voltammogram.

1.2.3.2 Chronoamperometry (CA)

The CA is a commonly used technique for determining diffusion coefficients and for investigating kinetics and mechanisms of the electrochemical reactions.[44] There are two types of commonly used chronoamperometry: *i.e.* controlled-potential CA and controlled-current CA, which is suitable for qualitative and quantitative analysis, respectively. In the ECR of CO_2, the controlled-potential CA was selected to study the effects of the potentials on the ECR of CO_2 in the presence of the electrocatalysts, to determine the faradaic efficiency by coupling with the CO_2 reduction product analysis setup and to investigate the stability of the electrocatalysts.[15] Before running controlled-potential CA, the electrochemical behavior of the analytes should be determined by CV first. After obtaining the appropriate reduction potential of the analytes, controlled-potential CA is performed by applying the constant potential chosen for the reaction for a certain period of time. **Figures 1-6a** and **1-6b** show a general potential excitation waveform and the resulting current response, respectively, from the controlled-potential CA study. This response

applies for semi-infinite linear diffusion; that is, with an unstirred solution and linear diffusion to the planar electrode with a supporting electrolyte to ensure the absence of ion migration and no other reactions. Similar to the CV, the equipment required to perform controlled-potential CA consists of the potentiostat coupled with the WE, CE and RE, which are submerged in the electrolyte sample solution.[45]
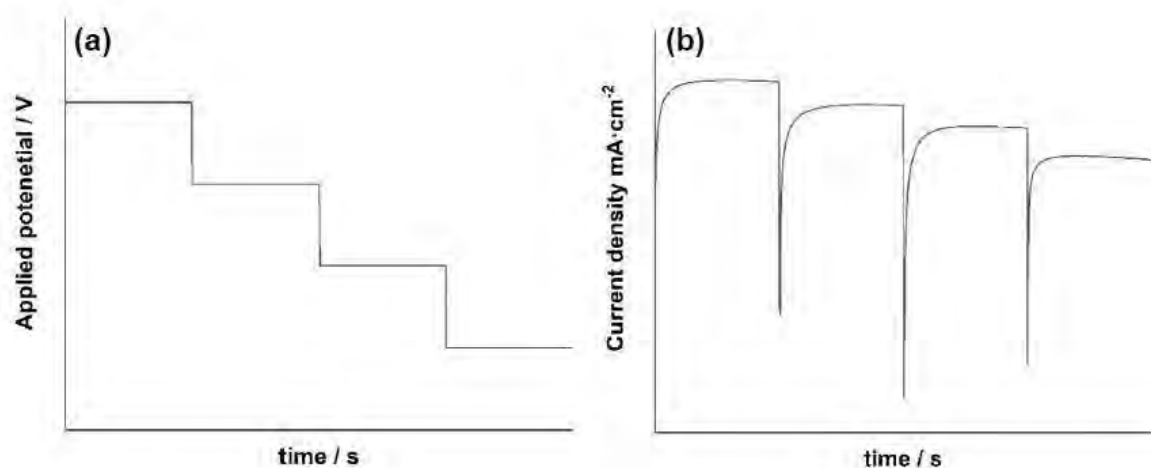
Figure 1-6: (a) A waveform and (b) current response obtained from CA.

1.2.4 Gas Chromatography (GC)

The GC is a common type of chromatography used for separating and analyzing compounds that can be vaporized without decomposition.[46] The GC is popular for environmental monitoring and industrial applications because it is very reliable and can be run nearly continuously.[47] It is also typically used in applications where small, volatile molecules are detected and with non-aqueous solutions. Typical uses of the GC include testing the purity of a particular substance or separating and quantifying components in a mixture. In some situations, the GC may help in identifying types of compounds. For the ECR of CO_2, the product can be analyzed by the GC both quantitatively and qualitatively. The gas products can be identified in the graph called "chromatogram", showing the peaks of all components in the gas sample injected to a GC instrument. Elution order in the GC depends on two factors: the boiling point of the solutes, and the interaction between the gases and the stationary phase, and is reported in terms of retention time (R_t). For the product analysis in this work, the products mainly detected are H_2, CO and CH_4, R_t of which was previously reported as shown in **Figure 1-7.**[48]
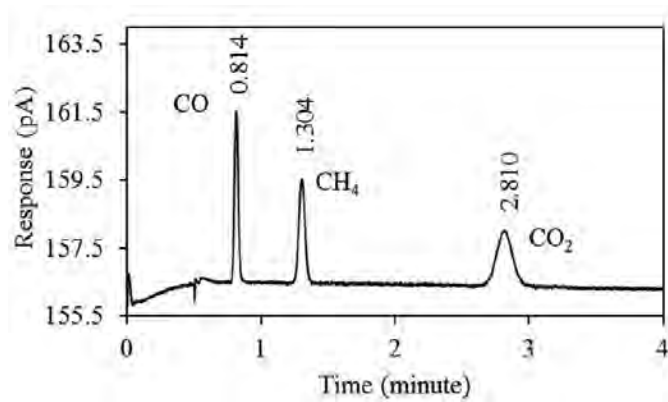
Figure 1-7: A exemplary gas chromatogram showing gaseous components at different R_f as reported by Harry Budiman and Oman Zuas[48]

Chapter II

Experiments

2.1 Synthesis

2.1.1 Materials and methods

All chemicals used in this work were purchased from commercial sources and used as received without further purification, unless noted otherwise.

Mass spectra were obtained using matrix-assisted laser desorption ionization time-of-flight (MALDI-TOF) mass spectrometry with dithranol or α-cyano-4-hydroxy cinnamic acid (α-CCA) as a matrix.

2.1.2 Synthesis of 2,9,16,23-tetraaminophthalocyaninatocobalt(II) (CoTAPc), 2,9,16,23-tetraaminophthalocyaninatonickel(II) (NiTAPc) and 2,9,16,23-tetraaminophthalocyaninatocopper(II) (CuTAPc) complex
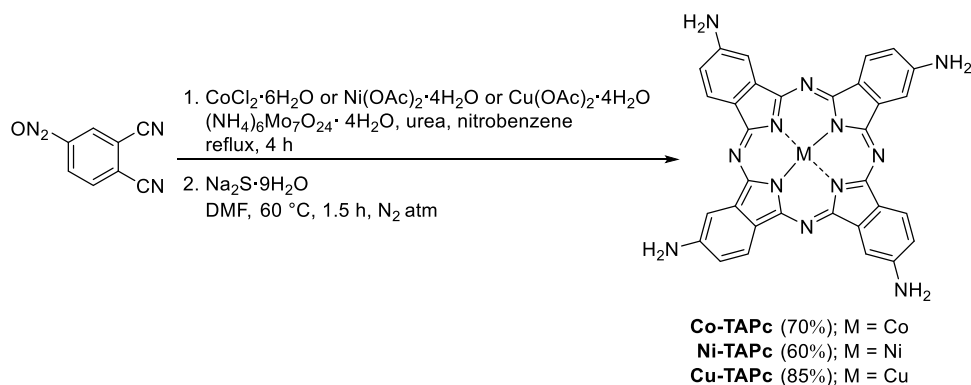
Figure 2-1: Synthesis procedure for the target compounds

Following a published procedure,[49] a solution of nitrophthalonitrile (865 mg, 5.00 mmol) in nitrobenzene (25 mL) was reacted with Cu(OAc)$_2$·H$_2$O (250 mg, 1.25 mmol), CoCl$_2$·6H$_2$O (300 mg, 1.25 mmol) or Ni(OAc)$_2$·4H$_2$O (310 mg, 1.25 mmol) in a presence of (NH$_4$)$_6$Mo$_7$O$_{24}$·4H$_2$O (60 mg, 0.050 mmol) and urea (1500 mg, 25.00 mmol) under reflux for 4 h. After the reaction mixture was cooled to room temperature, toluene (75 mL) was added. The resulting precipitate was collected by centrifugation, and washed with toluene, water, methanol:diethyl ether (1:9) and

then ethyl acetate:hexanes (2:1). The precipitate was dissolved in DMF and reacted with Na$_2$S·9H$_2$O under N$_2$ atmosphere at 60 °C for 1.5 h. Then, the mixture was diluted with water (75 mL) and then the pH was adjusted to 7 by adding concentrated HCl. Finally, the precipitate was collected by centrifugation and washed with methanol:diethyl ether (1:9) to obtain **CoTAPc**, **NiTAPc** or **CuTAPc** as dark green powder.

CoTAPc (550 mg, 70 %). *m/z* (%): found, 631.198 (100) [M$^+$]; calcd, 631.127 (M$^+$; M= C$_{32}$H$_{20}$N$_{12}$Co)

NiTAPc (471 mg, 60 %). *m/z* (%): found, 630.449 (100) [M$^+$]; calcd, 630.129 (M$^+$; M= C$_{32}$H$_{20}$N$_{12}$Ni)

CuTAPc (675 mg, 85 %). *m/z* (%): found, 635.238 (100) [M$^+$]; calcd, 635.123 (M$^+$; M= C$_{32}$H$_{20}$N$_{12}$Cu)

2.2 Electrochemical reduction (ECR) of CO$_2$

2.2.1 Background current (Blank solution)

A background cyclic voltammogram was achieved in a three-electrode one-compartment cell by using a 0.1 M tetrabutylammonium hexafluorophosphate (TBAPF$_6$) solution in DMF with 3% v/v water (10 mL) as an electrolyte solution. A glassy carbon electrode was used as the WE whereas a Pt plate served as the CE. A silver wire coated with silver chloride (Ag/AgCl) was used as a quasi-reference electrode (QRE), which was prepared by a published method.[50] The Ag/AgCl QRE was externally calibrated with a ferrocene/ferrocenium redox couple (~3mg) using a potential of 0.36 V vs. a normal hydrogen electrode (NHE) as a reference value.[51] The cyclic voltammograms were recorded at the potential range from 0.00 V to −1.60 V vs. a Ag/AgCl QRE at the scan rate of 50 mV·s^{-1} with a number of scanning cycles of 5. Thereby, the potential values were reported with respect to the Ag/AgCl QRE. Before each experiment, the solution was purged with either nitrogen (N$_2$) or CO$_2$ for 15 min.

2.2.2 Study of the ECR of CO_2 by cyclic voltammetry

The electrochemical properties and catalytic activities of the target MPc derivatives towards the   homogeneous ECR of CO_2 was performed by means of CV in a 0.1 M TBAPF$_6$ solution in DMF containing 0.5 mM **CoTAPc**, **NiTAPc** or **CuTAPc** and 3% v/v H_2O in the three-electrode one-compartment system. The glassy carbon was used as the WE, the Pt plate was used as the CE and the Ag/AgCl QRE was used. The cyclic voltammograms were recorded at the potential ranging from 0.00 V to -1.60 V vs. Ag/AgCl QRE at the scan rate of 50 mV·s^{-1} with the number of scanning cycles of 5. Thereby, the potential values were reported with respect to the Ag/AgCl QRE. The solutions were purged with either N_2 or CO_2 for 15 min prior to each experiment.

2.2.3 Study of the ECR of CO_2 by chronoamperometry and gas chromatography

Controlled potential electrolysis (CPE) of the target MPc was performed at ambient temperature using the above-mentioned electrochemical setup and at an applied potential of -1.60 V. After 2 h, a headspace (2 mL) gas sample from headspace gas (total volume of 11 mL) was collected from the electrochemical cell and then analyzed by gas chromatography (GC) equipped with a thermal conductivity detector (TCD).

Chapter III

Results and Discussion

3.1 Synthesis and Characterization of Target Phthalocyanines

Synthesis of **CoTAPc**, **NiTAPc** and **CuTAPc**, shown in **Scheme 3-1**, started from phthalocyanine ring formation and simultaneous metalation by a reaction of 4-nitrophtalonitrile under catalysis of ammonium molybdate in the presence of urea and $CoCl_2 \cdot 6H_2O$, $Ni(OAc)_2 \cdot 4H_2O$ or $Cu(OAc)_2 \cdot H_2O$, respectively. After that, the resulting tetranitrophthalocyanine complexes were reduced by $Na_2S \cdot 9H_2O$, leading to **CoTAPc**, **NiTAPc** and **CuTAPc** in 70%, 60% and 85% overall yield, respectively.
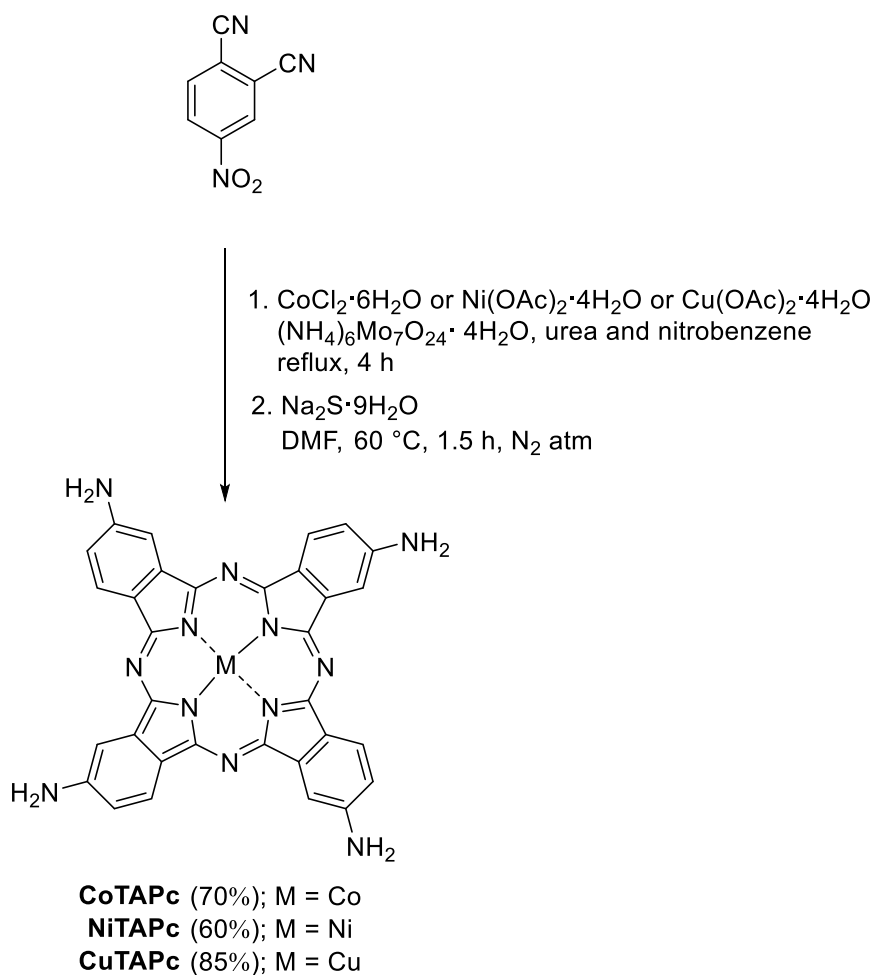
Scheme 3-1: Synthesis of target compounds

Scheme 3-2 illustrates the mechanism[52] of the formation of phthalocyanine ring and metalation. To begin with, ammonia was generated by the degradation of urea and then attacked 4-nitrophthalonitrile to form 4-nitrodiiminoisoindoline. After that, the formation of phthalocyanine ring and metalation occurred simultaneously. Reduction of phthalocyanine complexes were carried out by using $Na_2S \cdot 9H_2O$ to achieve target compounds.

(1) Degradation of Urea

Isocyanic acid
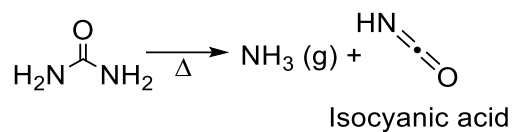
(2) Formation of diiminoisoindoline (Ammonolysis of Phthalonitrile)

diiminoisoindoline
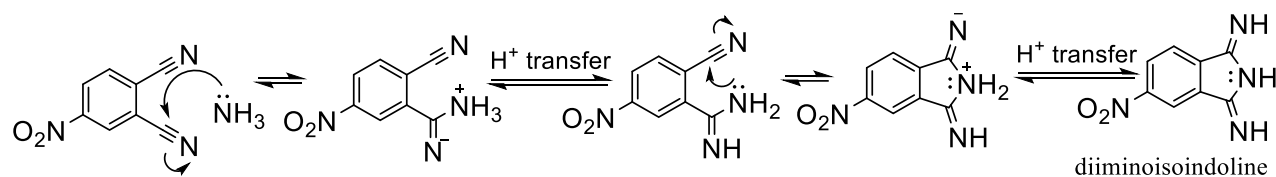
(3) Formation of Phthalocyanine Ring and Metalation
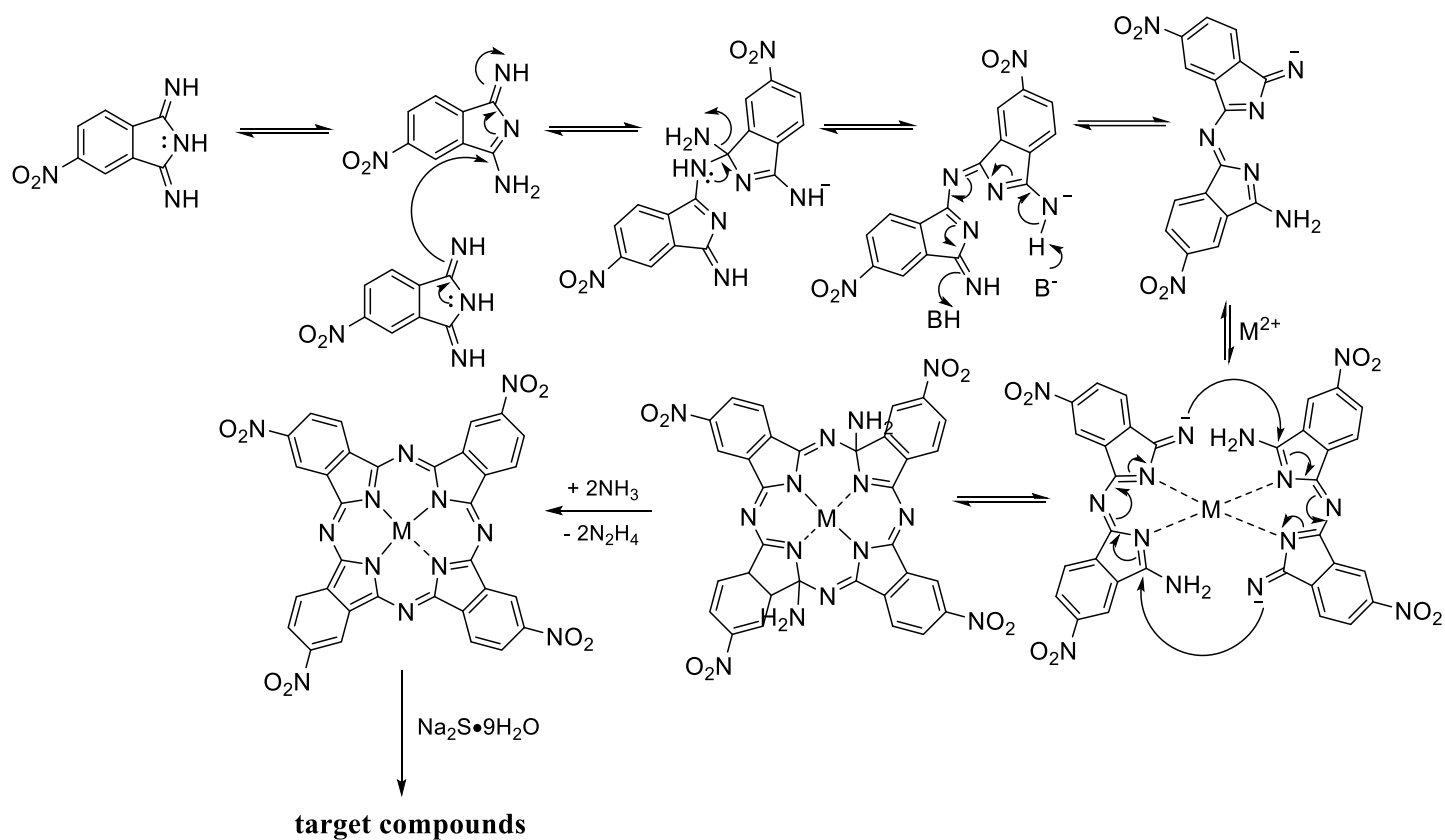
target compounds

Scheme 3-2: Proposed mechanism[52] of the synthesis of target compounds

Successful formation of the target compounds was confirmed by MALDI-TOF mass spectrometry exhibiting their molecular ion peaks at m/z of 631.198, 630.449 and 635.238 for **CoTAPc**, **NiTAPc** and **CuTAPc**, respectively. (**Figures 3-1**) However, the purity of products could not be determined by the spectra obtained from this technique.
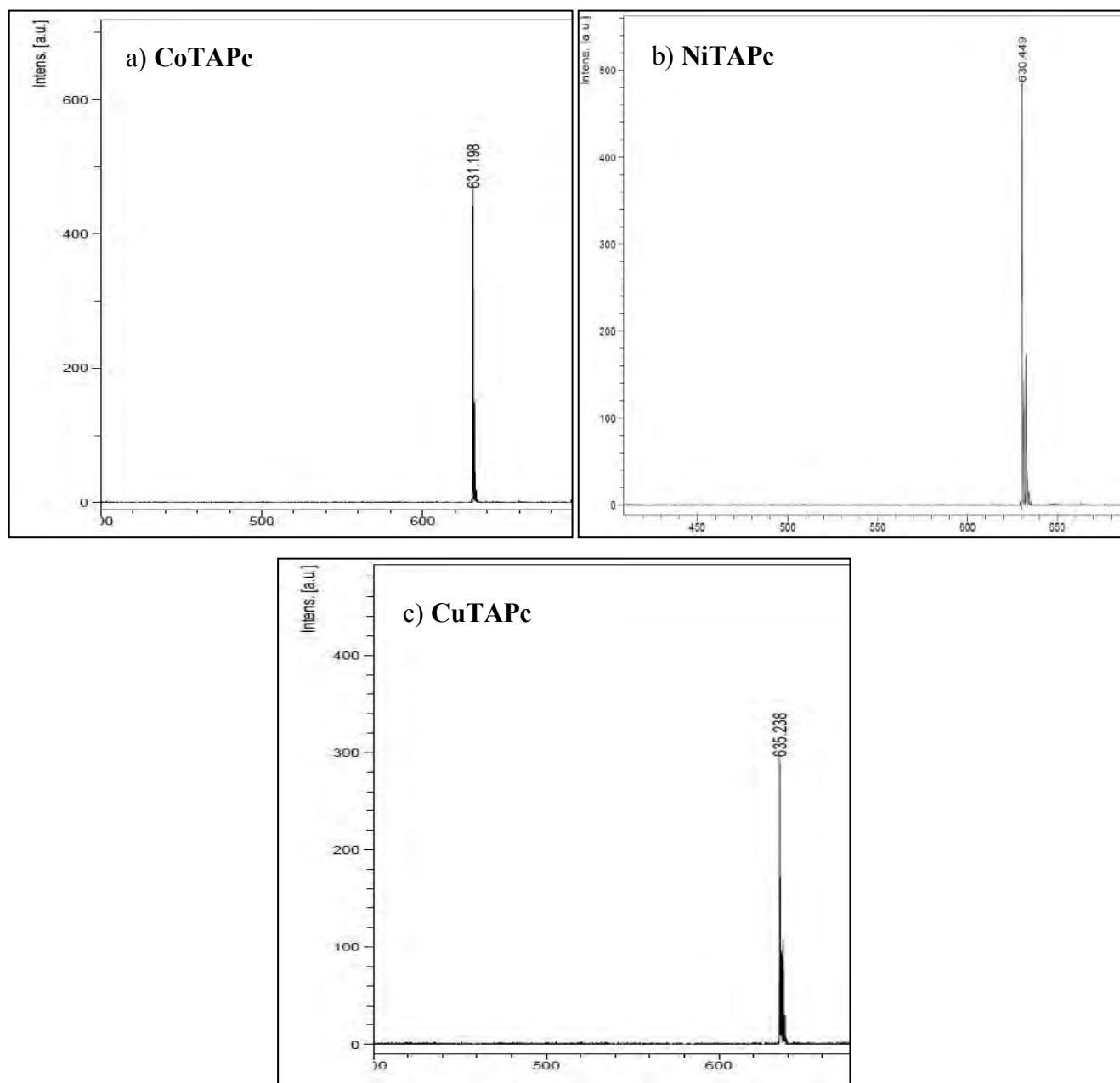
Figure 3-1: Mass spectra of a) **CoTAPc** b) **NiTAPc** c) **CuTAPc**

3.2 Electrochemical Studies of Target Phthalocyanines

3.2.1 Calibration of a Ag/AgCl Quasi-reference Electrode

External calibration of the Ag/AgCl QRE was achieved in a three-electrode one-compartment cell with a N_2-purged solution of 0.1 M tetrabutylammonium hexafluorophosphate (TBAPF$_6$) solution in anhydrous DMF containing ferrocene (Fc). The cyclic voltammogram was recorded at the potential range from 0.00 V to 0.80 V vs. Ag/AgCl QRE at the scan rate of 50 mV·s^{-1} with a number of scanning cycles of 3. **Figure 3-2** demonstrates a unique "Duck" shape cyclic voltammogram with an anodic peak at 0.44 V and a cathodic peak at 0.36 V for the forward and reverse scans, respectively. Therefore, an experimental half potential ($E_{1/2}$) value for a Fc/Fc$^+$ redox couple was 0.40 V, which is the same as the literature value reported.[53] Consequently, the potential values in this work were reported with respect to the Ag/AgCl QRE.
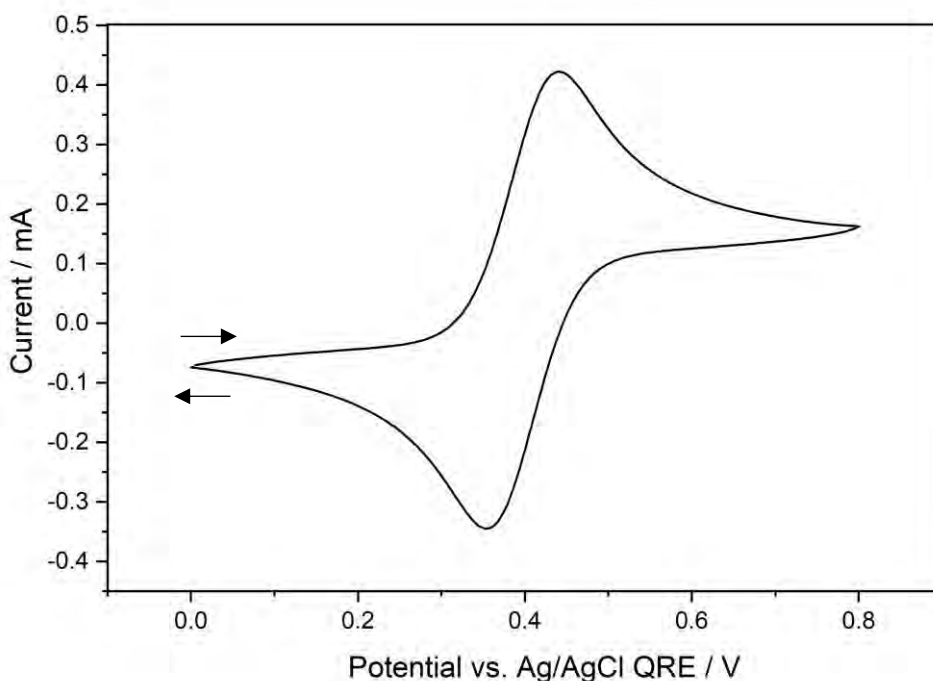
Figure 3-2: A cyclic voltammogram of a ferrocene/ferrocenium redox couple

3.2.2 Investigation of Electrochemical Behaviors and Catalytic Activities of MPc derivatives towards Homogeneous CO$_2$ Reduction by Cyclic Voltammetry

In this study, the electrochemical behaviors and catalytic activities of **CoTAPc**, **Ni-TAPc** and **CuTAPc** towards the CO$_2$ reduction were investigated by the CV using the three-electrode one-compartment setup consisting of the glassy carbon as the WE, the Pt plate as the CE and the Ag/AgCl QRE. The cyclic voltammograms were recorded in a DMF solution containing 0.5 mM **CoTAPc**, **Ni-TAPc** or **CuTAPc**, 3% v/v H$_2$O as a proton source and 0.1 M TBAPF$_6$ as the supporting electrolyte at the potential range from 0.00 V to −1.60 V vs. Ag/AgCl QRE at a scan rate of 50 mV·s^{-1} for 3 cycles. The solutions were purged with N$_2$ for 15 min prior to each measurement to investigate the electrochemical behaviors of the target compounds. Afterwards, the solutions were purged with CO$_2$ for 15 min to study for their electrocatalytic activities for ECR of CO$_2$. As shown in **Figure 3-3a**, the N$_2$-saturated **CoTAPc** solution gave quasi-reversible reduction peaks at peak potentials (E$_{peak}$) of −0.58 V and −1.34 V vs. Ag/AgCl QRE, corresponding to Co^{II}/Co^{I} and phthalocyanine ring reduction,[53] respectively. In addition, two small reduction peaks at −1.05 V and −1.25 V vs Ag/AgCl QRE, which were not consistent with the reduction of **CoTAPc,** were merely observed under N$_2$-saturated condition, indicating the presence of other unknown electroactive species in the solution. Under the CO$_2$ condition, the first reduction peaks were observed at a similar E$_{peak}$, −0.57 V vs Ag/AgCl QRE, with a small decrease in current compared with that observed under the N$_2$-saturated condition. This observation suggested that the first reduction did not involve in the catalytic CO$_2$ reduction. In contrast, the second reduction peak was observed with a slight positive shift to −1.26 V vs Ag/AgCl QRE and significant increase in current from 200 µA to 275 µA, compared with the current observed under the N$_2$-saturated condition, indicating that **CoTAPc** might promote the ECR of CO$_2$ at the potential over −1.26 V vs. Ag/AgCl QRE.
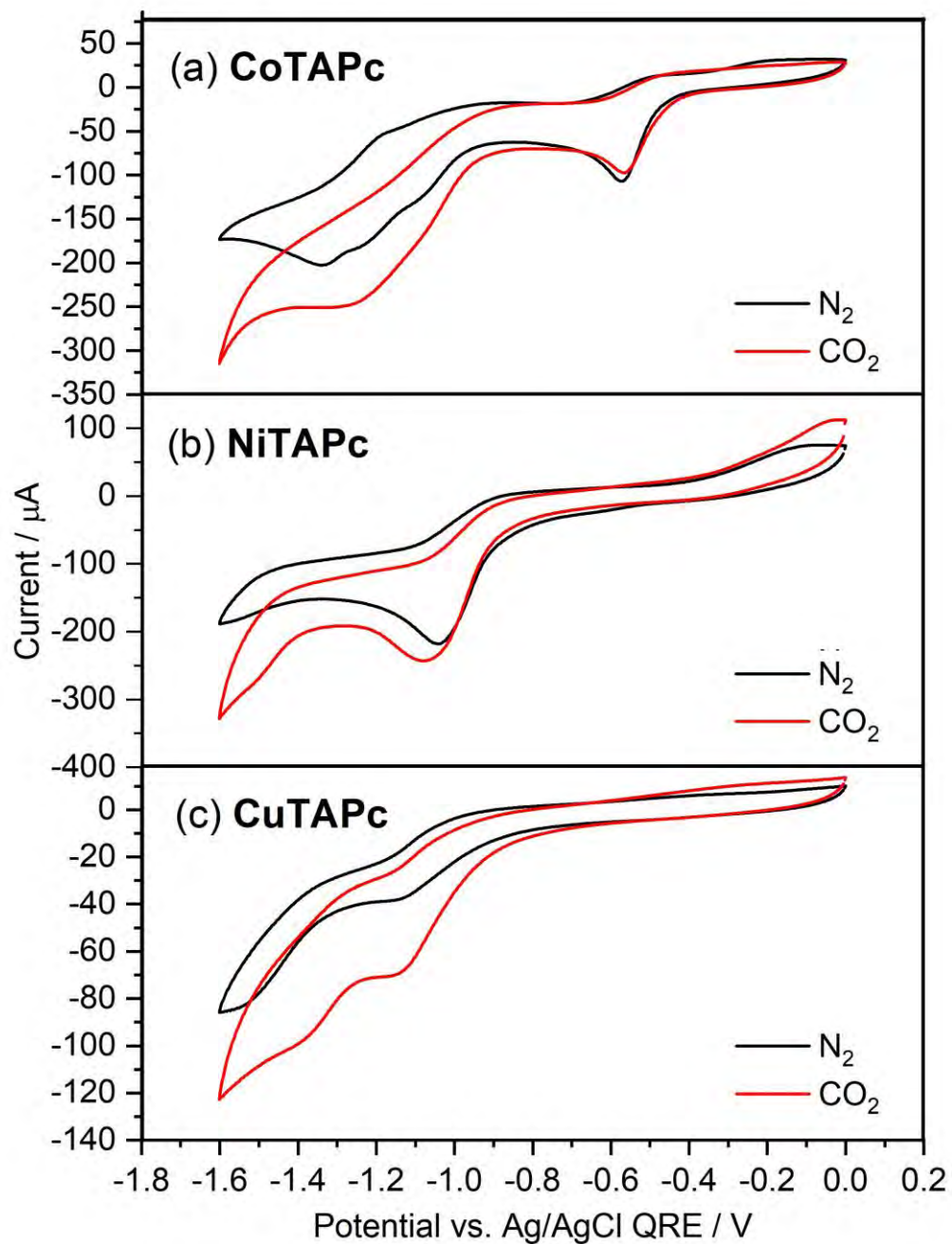
Figure 3-3: Cyclic voltammograms of TBAPF$_6$ solutions in DMF containing 3% v/v H$_2$O and 0.5 mM a) **CoTAPc**, b) **NiTAPc** and c) **CuTAPc** under N$_2$ (black solid line) and CO$_2$ atmosphere (red solid line)

In a similar manner, under the N_2 atmosphere, **NiTAPc** exhibited two quasi-reversible peaks at −1.04 V and−1.51 V vs. Ag/AgCl QRE (**Figure 3-3b**). As reported in a published literature,[54] the processes occurring at −1.04 V and −1.50 V could be assigned to the Pc^{2-}/Pc^{3-} and Pc^{3-}/Pc^{4-} redox couple, respectively, indicating only the reduction of phthalocyanine ring. Under the CO_2 saturated, two reduction peaks were observed at −1.10 V and −1.49 V vs Ag/AgCl QRE with the significant current enhancement at the second one where the current was increased from 190 μA to 330 μA. This observation suggested that **NiTAPc** might promote the ECR of CO_2 at the potential of −1.49 V vs. Ag/AgCl QRE or higher.

According to **Figure 3−3c**, the N_2-saturated **CuTAPc** solution provided two quasi-reversible reduction peaks at −1.14 V and −1.50 V vs. Ag/AgCl QRE, corresponding to reduction processes of the phthalocyanine ring.[55] Under the CO_2 saturation, the first reduction peak was observed at the same potential but the current was significantly increased, compared with that observed under the N_2-saturated condition, from 40 μA to 78 μA. This observation suggested that the first reduction might involve in the catalytic CO_2 reduction. The second reduction peak was observed with a positively significant shift to −1.35 V vs Ag/AgCl QRE with significant increase in current from 80 μA to 110 μA. The results indicated that **CuTAPc** might be able to promote the ECR of CO_2 at the potential over −1.14 V vs. Ag/AgCl QRE. Moreover, the reason why the current measured in the solution of **CuTAPc** was the least current compared to those of **CoTAPc** and **NiTAPc** can be explained the limited solubility of **CuTAPc**. Although the amount of **CuTAPc** was exactly measured to prepare a solution with the same concentration as others, it did not efficiently dissolve to achieve an absolute homogenous solution and did not give the expected concentration. Therefore, to improve the solubility, the sonication time should be longer to assure that **CuTAPc** was completely dissolved.

All reduction peak potentials with their currents were summarized in **Table 3-1,** along with percent current enhancement at -1.6 V vs. Ag/AgCl QRE of each catalyst, which can be calculated by equation (1) :

% current enhancement

$$= \frac{\text{Current observed under } CO_2 \text{atmosphere} - \text{ Current observed under } N_2 \text{atmosphere}}{\text{Current observed under } N_2 \text{atmosphere}} \times 100 \quad (1)$$

The result showed that **CoTAPc** might be the most promising catalyst for the ECR of CO_2 with the highest % current enhancement of 77 %.

Table 3-1: Catalytic performance of **CoTAPc**, **NiTAPc** and **CuTAPc** for homogeneous ECR of CO_2.

Compound	Condition	E_{peak} / V (current / μA) vs. Ag/AgCl QRE	Current at -1.6 V vs. Ag/AgCl QRE / μA	Percent current enhancement at -1.6 V vs. Ag/AgCl QRE / %
CoTAPc	N_2	-0.58 (110), -1.34 (200)	175	77
	CO_2	-0.57 (108), -1.26 (275)	310	
NiTAPc	N_2	-1.04 (220), -1.51 (180)	190	74
	CO_2	-1.10 (240), -1.49 (290)	330	
CuTAPc	N_2	-1.14 (40), -1.50 (80)	85	44
	CO_2	-1.14 (78), -1.35 (110)	122	

The cyclic voltammogram of the glassy carbon electrode in the blank solution in the absence of MPc derivatives showed no redox peak with the slight current enhancement under the CO_2 saturated condition (**Figure 3−4**). However, this current enhancement can be ignored due to a very small value of current, compared with that observed in the case where the MPc compounds were present. This experiment confirmed that the current enhancement of solution with MPc compounds actually came from the catalytic activity of ECR of CO_2.
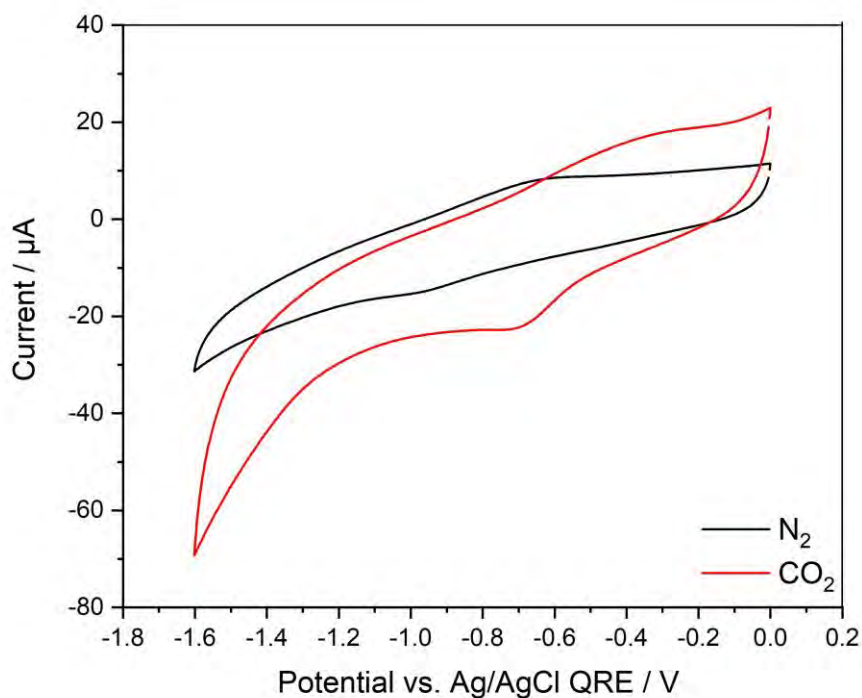
Figure 3-4 : A cyclic voltammogram of a glassy carbon under N_2 (black solid line) and CO_2 atmosphere (red solid line)

According to the reduction peak potentials and the significant current enhancement obtained from the CV in the presence of MPc derivatives, the reduction potential of −1.6 V vs. Ag/AgCl QRE was chosen for the controlled-potential CA due to its maximum current enhancement.

3.2.3 Reduction Product Analysis of Homogeneous CO_2 Reduction by Chronoamperometry and Gas Chromatography

The controlled-potential CA was performed for 2 h in the same three-electrode one-compartment setup as the above-mentioned CV experiments, except that the carbon paper was served as the WE due to its higher surface area than that of the glassy carbon electrode. Throughout the electrolysis, the solution must be stirred to give convection to the solution, resulting in the most efficient mass transfer of electroactive species to the electrode surface. The chronoamperograms of the ECR of CO_2 in the presence of **CoTAPc**, **NiTAPc** and **CuTAPc** were shown in **Figure 3-5**. At the beginning, a current dramatically increased until reached a maximum cathodic current of –2.1 mA and –3.0 mA for **CoTAPc**, **NiTAPc**, respectively and remained constant to the end of the experiment. However, the chronoamperogram of **CuTAPc** was different from the others. During the first 500 seconds of electrolysis of **CuTAPc**, the magnetic stirrer was accidently shut off, so the mass transfer did not occur effectively, providing less amount of current measured of –1.5 A. After stirring for 500 seconds, the stirrer was finally working again and the current was increased to –2.0 A as the convection was increased by the stirrer. A peak area indicating the amount of electricity used for the ECR of CO_2 was obtained by integrating each I·t curve in the chronoamperograms. The peak areas of 15,455.48 mA·s, 21,111.95 mA·s and 15,132.46 mA·s belonged to **CoTAPc**, **NiTAPc** and **CuTAPc**, respectively.
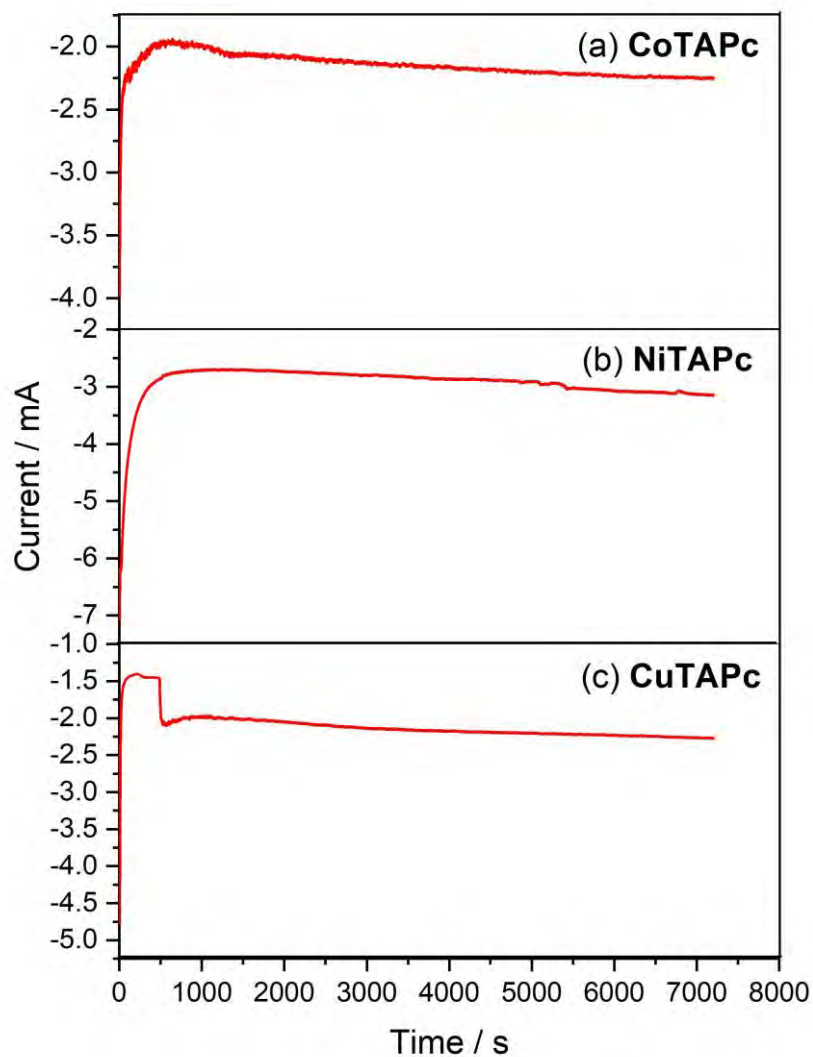
Figure 3-5 : Chronoamperograms of the ECR of CO_2 in the presence of a) **CoTAPc**, b) **NiTAPc** and c) **CuTAPc**

After 2h of CO_2 electrolysis, 2 mL of a gas sample was collected from the reaction vial having a headspace volume of 11 mL. The sample gas was then analyzed by gas chromatography (GC) equipped with a thermal conductivity detector (TCD).

Figure 3-6 represented chromatograms of gas samples collected from each solution of **CoTAPc**, **NiTAPc** and **CuTAPc**. The products from the ECR of CO_2 were H_2 and CO, which could be found in each chromatogram at retention time (t_R) of 0.609 min and 1.928 min, respectively. Other peaks found at t_R of 0.688 min and 0.856, about 4.67 min, 5.554 min and about 8.00 min corresponded to detection of O_2, N_2 ,permanent gases (H_2, O_2 N_2 and CO) and two peaks of CO_2, respectively. The column set used for GC analysis was a specific GC column called "Select Permanent Gases/CO_2", which consisted of two parallel columns containing CP-Molsieve 5Å for permanent gas analysis and CP-PoraBOND Q for CO_2 analysis. Therefore, this column set separated the permanent gases and CO_2 in a single run, while the CP-Molsieve could effectively separate the permanent gases but absorb CO_2. As a result, the 1st to 4th peaks were obtained from the separation of the permanent gases of the column containing CP-Molsieve, and the 5th one belonged to all permanent gases that could not be separated by CP-PoraBOND Q. The 6th and 7th peak corresponded to CO_2 detected by CP-PoraBOND Q and retained CO_2 from CP-Molsieve 5Å, respectively. According to the chromatogram of H_2, the signal was detected as a negative peak because H_2 has a small difference in thermal conductivity compared to helium carrier gas.
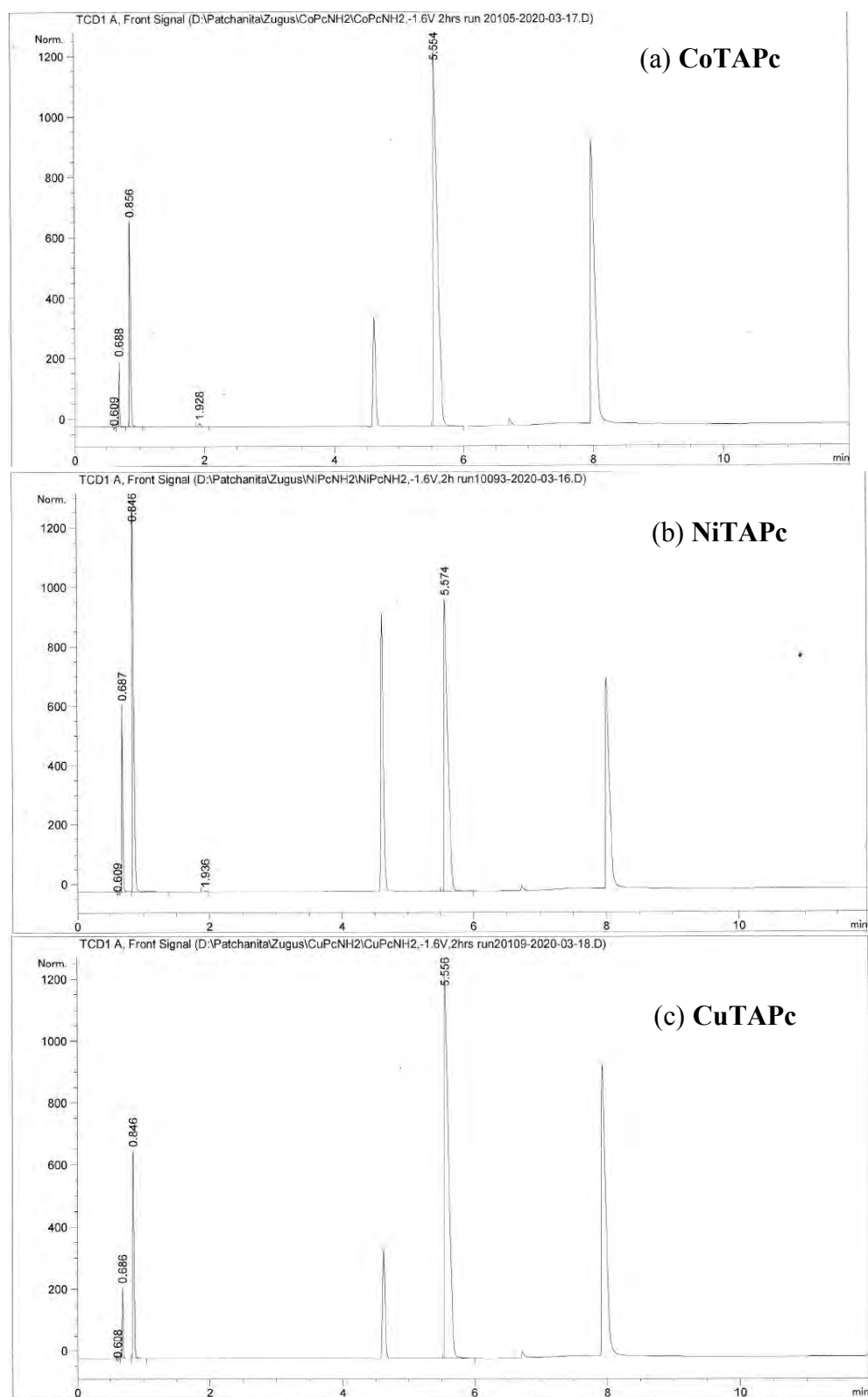
Figure 3-6: Chromatograms of gas samples collected from the electrochemical cell of the ECR of CO_2 in the presence of a) **CoTAPc**, b) **NiTAPc** and c) **CuTAPc**

The information obtained from GC was all presented in **Table 3-2**, including a retention time (t_R), the type of gas and the peak area of reduction products: hydrogen gas (H_2) and carbon monoxide (CO).

Table 3-2: Retention times (t_R) of the gas component detected from the ECR of CO_2 in the presence of a) **CoTAPc**, b) **NiTAPc** and c) **CuTAPc** by GC

Compound	Retention time (t_R) / min						
	1st peak H_2	2nd peak O_2	3rd peak N_2	4th peak **CO**	5th peak permanent gases	6th peak CO_2	7th peak CO_2
a) **CoTAPc**	0.609	0.688	0.856	1.928	About 4.67	5.554	About 8.00
b) **NiTAPc**	0.609	0.687	0.846	1.936		5.574	
c) **CuTAPc**	0.608	0.686	0.846	*N/A		5.556	

% Faradaic efficiency (% FE) can be calculated by following the step provided below.

The headspace volume of 11 mL was calibrated by real volume of gas in head space without including the volume of electrodes. Therefore, with the peak area calibrated by standard gas from GC, the volume of CO or H_2 could be calculated by equation (2).

$$\text{Volume of CO or } H_2 = \text{Headspace volume (11 mL)} \times \text{\% Peak area of CO or } H_2 \qquad (2)$$

With the volume of CO or H_2, we could simply calculate both mol CO and mol H_2 ,respectively, by the ideal gas law.

$$n = \frac{PV}{RT}$$

$$\text{mol CO or mol H}_2 = \frac{(1\ \text{atm})(\text{Volume of measured gas from (2)} \times\ 10^{-3}\ \text{L})}{(0.08206\ \text{L} \cdot \text{atm/mol} \cdot \text{K})(298\ \text{K})} \tag{3}$$

According to the equation (4) and (5), the total number of moles of electron output for CO and H_2 was calculated by equation (6), respectively.

$$CO_2 + 2H^+ + 2e^- \longrightarrow CO + H_2O \tag{4}$$

$$2H^+ + 2e^- \longrightarrow H_2 \tag{5}$$

$$\text{mol e}^-\text{output} = (\text{mol CO or mol H}_2 \text{ from (3)}) \times \frac{2\ \text{mol e}^-}{1\ \text{mol CO or mol H}_2} \tag{6}$$

The total number of moles of electrons input measured during the ECR of CO_2 can be calculated by Faraday's law of electrolysis (7)

$$\text{mol e}^-\text{input} = \frac{Q}{F} = \frac{It}{F} = \frac{\text{Peak area of I} \cdot \text{t curve (C)}}{\text{Faradic constant (96485 C/mol e}^-)} \tag{7}$$

Accordingly, % FE was simply calculated by equation (8)

$$\%\ \text{FE}\ = \frac{\text{mol e}^-\text{output}}{\text{mol e}^-\text{input}} \times 100\% \tag{8}$$

The experimental data for the calculation of % FE together with % FE of H_2 and CO_2 was reported in **Table 3-3**.

Table 3-3: Catalytic performance of **CoTAPc**, **NiTAPc** and **CuTAPc** for the ECR of CO_2

Compound	% Peak area of H_2	% Peak area of CO	Peak area of I·t curve / mA·s	% H_2	Volume of H_2 / mL	% FE of H_2	%CO	Volume of CO / mL	% FE of CO
CoTAPc	5.66466	0.280314	15455.48	5.66466	0.62	31.80	0.280314	0.03	1.57
NiTAPc	8.45481	0.0459514	21111.95	8.45481	0.93	34.74	0.0459514	0.01	0.19
CuTAPc	6.72659	N/A	15132.46	6.72659	0.74	38.57	N/A	N/A	N/A

[*]N/A : the product was not found.

Considering the catalytic performance of the target compounds for the ECR of CO_2 in terms of % FE, it can be concluded that the **CoTAPc** showed the highest catalytic activity followed by **NiTAPc** and **CuTAPc**, respectively. Unfortunately, the main product was H_2, which possibly came from the hydrogen evolution due to the presence of H_2O in the solution. In addition, the electrochemical cell used for the ECR of CO_2 consisted of the WE and the CE in the same set up, which might cause the reversed oxidation of CO_2 at the surface of the CE, resulting in the low amount of CO occurred from the reaction. To improve % FE of CO, the WE and the CE should be completely separated from each other by using more effective electrochemical set up to assure that all CO molecules produced at the WE would not go to react at the surface of the CE. Even though **CuTAPc** demonstrated the highest % FE of H_2, it was still not a suitable catalyst for the ECR of CO_2 because there was no CO produced by the ECR of CO_2 with the presence of **CuTAPc**. Therefore, the most promising candidates for future studies were **CoTAPc** and **NiTAPc**, respectively.

Chapter IV

Conclusion

The cobalt, nickel and copper complexes of 2,9,16,23-tetraaminophthalocyaninatocobalt(II), -nickel(II) and −copper(II), *i.e.* **CoTAPc**, **NiTAPc** and **CuTAPc**, respectively, were successfully synthesized by a two-step procedure in 70, 60 and 85% overall yield, respectively. Investigation of their electrochemical behaviors and catalytic performance towards the homogeneous ECR of CO_2 by means of CV showed that, at the potential of −1.6 V, **CoTAPc** exhibited the greatest current enhancement of 77%. In addition, CV provided qualitative information of the electroactive species by their reduction potentials, which could be used as an identification tool. The catalytic performance of the target compounds was further investigated *via* electrolysis by means of the controlled-potential CA, together with the product analysis by the GC. The results showed that, of all complexes, **CoTAPc** gave the highest %FE for both H_2 and CO formations, *i.e.* 32% and 1.6%, respectively, while **CuTAPc** could yield only H_2. Although the CO formation was observed in these studies, yield suppression due to strong competition from H_2 generation by the water splitting process still has to be overcome. Accordingly, the optimization of the ECR condition and setup, *i.e.* the use of two-compartment cell to separate the WE and the CE, the modification of either the WE or the chemical structures of catalysts should be further studied to increase the efficiency of the ECR of CO_2 and will be described elsewhere.

References

1. Davis, S. J.; Caldeira, K.; Matthews, H. D., Future CO_2 emissions and climate change from existing energy infrastructure. *Science* **2010,** *329* (5997), 1330-1333.

2. Trenberth, K. E.; Dai, A.; Van Der Schrier, G.; Jones, P. D.; Barichivich, J.; Briffa, K. R.; Sheffield, J., Global warming and changes in drought. *Nat. Clim. Change.* **2014,** *4* (1), 17-22.

3. Maginn, E. J., What to do with CO_2. *J. Phys. Chem. Lett.* **2010,** *1* (24), 3478−3479.

4. Owusu, P. A.; Asumadu-Sarkodie, S., A review of renewable energy sources,sustainability issues and climate change mitigation. *Cogent Eng.* **2016,** *3* (1), 1167990-1168003.

5. Yu, C. H.; Huang, C. H.; Tan, C. S., A review of CO_2 capture by absorption and adsorption. *Aerosol Air Qual. Res.* **2012,** *12* (5), 745-769.

6. Khezri, B.; Fisher, A. C.; Pumera, M., CO_2 reduction: the quest for electrocatalytic materials. *J. Mater. Chem. A* **2017,** *5* (18), 8230-8246.

7. Kuhl, K. P.; Hatsukade, T.; Cave, E. R.; Abram, D. N.; Kibsgaard, J.; Jaramillo, T. F., Electrocatalytic conversion of carbon dioxide to methane and methanol on transition metal surfaces. *J. Am. Chem. Soc.* **2014,** *136* (40), 14107-14113.

8. Rosen, B. A.; Salehi-Khojin, A.; Thorson, M. R.; Zhu, W.; Whipple, D. T.; Kenis, P. J. A.; Masel, R. I., Ionic liquid-mediated selective conversion of CO_2 to CO at low overpotentials. *Science* **2011,** *334* (6056), 643-644.

9. Hori, Y., Electrochemical CO2 reduction on metal electrodes. In *Modern Aspects of Electrochemistry*, Vayenas, C. G.; White, R. E.; Gamboa-Aldeco, M. E., Eds. Springer New York: New York, NY, **2008**; 89-189.

10. Huo, S.; Weng, Z.; Wu, Z.; Zhong, Y.; Wu, Y.; Fang, J.; Wang, H., Coupled metal/oxide catalysts with tunable product selectivity for electrocatalytic CO_2 reduction. *ACS Appl. Mater. Interfaces* **2017,** *9* (34), 28519-28526.

11. Zhou, B. W.; Song, J. L.; Xie, C.; Chen, C. J.; Qian, Q. L.; Han, B. X., Mo-Bi-Cd ternary metal chalcogenides: Highly efficient photocatalyst for CO_2 reduction to formic acid under visible light. *ACS Sustain. Chem. Eng.* **2018,** *6* (5), 5754–5759.

12. Wu, J.; Yadav, R. M.; Liu, M.; Sharma, P. P.; Tiwary, C. S.; Ma, L.; Zou, X.; Zhou, X.-D.; Yakobson, B. I.; Lou, J., Achieving highly efficient, selective, and stable CO_2 reduction on nitrogen-doped carbon nanotubes. *ACS nano.* **2015,** *9* (5), 5364-5371.

13. Kumar, B.; Asadi, M.; Pisasale, D.; Sinha-Ray, S.; Rosen, B. A.; Haasch, R.; Abiade, J.; Yarin, A. L.; Salehi-Khojin, A., Renewable and metal-free carbon nanofiber catalysts for carbon dioxide reduction. *Nat. Commun.* **2013,** *4*, 2819-2826.

14. Kornienko, N.; Zhao, Y.; Kley, C. S.; Zhu, C.; Kim, D.; Lin, S.; Chang, C. J.; Yaghi, O. M.; Yang, P., Metal–organic frameworks for electrocatalytic reduction of carbon dioxide. *J. Am. Chem. Soc.* **2015,** *137* (44), 14129-14135.

15. Zhang, X.; Wu, Z.; Zhang, X.; Li, L.; Li, Y.; Xu, H.; Li, X.; Yu, X.; Zhang, Z.; Liang, Y., Highly selective and active CO_2 reduction electrocatalysts based on cobalt phthalocyanine/carbon nanotube hybrid structures. *Nat. Commun.* **2017,** *8*, 14675-14683.

16. Kusama, S.; Saito, T.; Hashiba, H.; Sakai, A.; Yotsuhashi, S., Crystalline copper(II) phthalocyanine catalysts for electrochemical reduction of carbon dioxide in aqueous media. *ACS catal.* **2017,** *7* (12), 8382-8385.

17. Han, N.; Wang, Y.; Ma, L.; Wen, J.; Li, J.; Zheng, H.; Nie, K.; Wang, X.; Zhao,F.; Li, Y., Supported cobalt polyphthalocyanine for high-performance electrocatalytic CO_2 reduction. *Chem.* **2017,** *3* (4), 652-664.

18. Fukatsu, A.; Kondo, M.; Okabe, Y.; Masaoka, S., Electrochemical analysis of ironporphyrin-catalyzed CO_2 reduction under photoirradiation. *J. Photochem. Photobiol. A.***2015,** *313*, 143-148.

19. Sonkar, P. K.; Ganesan, V.; Gupta, R.; Yadav, D. K.; Yadav, M., Nickel phthalocyanine integrated graphene architecture as bifunctional electrocatalyst for CO_2 and O_2 reductions. *J. Electroanal. Chem.* **2018,** *826*, 1-9.

20. Isaacs, M.; Armijo, F.; Ramírez, G.; Trollund, E.; Biaggio, S.; Costamagna, J.; Aguirre, M. J., Electrochemical reduction of CO_2 mediated by poly-M-aminophthalocyanines (M= Co, Ni, Fe): poly-Co-tetraaminophthalocyanine, a selective catalyst. *J. Mol. Catal. A Chem.* **2005,** *229* (1-2), 249-257.

21. McKeown, N. B., Phthalocyanines. In Comprehensive Coordination Chemistry II, McCleverty, J. A.; Meyer, T. J., Eds. Pergamon: Oxford, **2003**; 507-514.

22. de la Torre, G.; Nicolau, M.; Torres, T., Chapter 1 - Phthalocyanines: Synthesis, Supramolecular Organization, and Physical Properties. In *Supramolecular Photosensitive and Electroactive Materials*, Nalwa, H. S., Ed. Academic Press: San Diego, **2001**; 1-111.

23. Tatyana N. L.; Elena Y. T.; New trends in the direct synthesis of phthalocyanine/porphyrin complexes., Elsevier: Monterrey, **2018**; 239-278.

24. Mack, J.; Stillman, M. J., 103 - Electronic Structures of Metal Phthalocyanine and Porphyrin Complexes from Analysis of the UV–Visible Absorption and Magnetic Circular Dichroism Spectra and Molecular Orbital Calculations. In The Porphyrin Handbook, Kadish, K. M.; Smith, K. M.; Guilard, R., Eds. Academic Press: Amsterdam, **2003**; 43-116.

25. Oni, J.; Ozoemena, K. I., Phthalocyanines in batteries and supercapacitors. *J. Porphyr. Phthalocyanines.* **2012,** *16* (07n08), 754-760.

26. Kuzyniak, W.; Schmidt, J.; Glac, W.; Berkholz, J.; Steinemann, G.; Hoffmann, B.; Ermilov, E. A.; Gürek, A. G.; Ahsen, V.; Nitzsche, B., Novel zinc phthalocyanine as a promising photosensitizer for photodynamic treatment of esophageal cancer. *Int. J. Oncol.* **2017,** *50* (3), 953-963.

27. Oteyza, D. G. d.; El-Sayed, A.; Garcia-Lastra, J. M.; Goiri, E.; Krauss, T. N.; Turak, A.; Barrena, E.; Dosch, H.; Zegenhagen, J.; Rubio, A.; Wakayama, Y.; Ortega, J. E., Copper-phthalocyanine based metal–organic interfaces: The effect of fluorination, the substrate, and its symmetry. *J. Chem. Phys.* **2010,** *133* (21), 214703-214708.

28. Milan, R.; Selopal, G. S.; Cavazzini, M.; Orlandi, S.; Boaretto, R.; Caramori, S.; Concina, I.; Pozzi, G., Dye-sensitized solar cells based on a push-pull zinc phthalocyanine bearing diphenylamine donor groups: computational predictions face experimental reality. *Sci. Rep.* **2017,** *7* (1), 15675.

29. Burkitt, R.; Whiffen, T.; Yu, E. H., Iron phthalocyanine and MnOx composite catalysts for microbial fuel cell applications. *Appl. Catal. B Environ.* **2016,** *181*, 279-288.

30. Muzikante, I.; Parra, V.; Dobulans, R.; Fonavs, E.; Latvels, J.; Bouvet, M., A novel gas sensor transducer based on phthalocyanine heterojunction devices. *Sensors.* **2007,** *7* (11), 2984 2996.

31. Dhavala, S. K.; Neelam, V. S. K.; Gideon, N., A review on fabrication of dye-sensitized solar cells. *Int. J. Adv. Res. Sci. Technol.* **2015,** *4*, 343-347.

32. Mohammed, H. A.; Kareem, M. M., Synthesis and characterization of new zincphthalocyanine with four dodecenyl-benzoic pendant groups. *JUBPAS.* **2017,** *25* (2), 496-486.

33. Sakamoto, K.; Ohno-Okumura, E., Syntheses and functional properties of phthalocyanines. *Materials* **2009,** *2* (3), 1127-1179.

34. Qiao, J. L.; Liu, Y. Y.; Hong, F.; Zhang, J. J., A review of catalysts for the electroreduction of carbon dioxide to produce low-carbon fuels. *Chem. Soc. Rev.* **2014,** *43* (2), 631-675.

35. Sridhar, N.; Hill, D.; Agarwal, A.; Zhai, Y.; Hektor, E., Carbon dioxide utilization. electrochemical conversion of CO_2–opportunities and challenges. *DNV. GL, Position Paper* **2011**.

36. Feng, D. M.; Zhu, Y. P.; Chen, P.; Ma, T. Y., Recent advances in transition-metalmediated electrocatalytic CO_2 reduction: from homogeneous to heterogeneous systems. *Catalysts.* **2017,** *7*, 373-391.

37. Lu, Q.; Jiao, F., Electrochemical CO_2 reduction: Electrocatalyst, reaction mechanism, and process engineering. *Nano Energy.* **2016,** *29*, 439-456.

38. Kumar, B.; Llorente, M.; Froehlich, J.; Dang, T.; Sathrum, A.; Kubiak, C. P., Photochemical and photoelectrochemical reduction of CO_2. *Annu. Rev. Phys. Chem.* **2012,** *63*, 541-569.

39. Sun, Z.; Ma, T.; Tao, H.; Fan, Q.; Han, B., Fundamentals and challenges of electrochemical CO_2 reduction using two-dimensional materials. *Chem.* **2017,** *3* (4), 560-587.

40. Elgrishi, N.; Rountree, K. J.; McCarthy, B. D.; Rountree, E. S.; Eisenhart, T. T.; Dempsey, J. L., A practical beginner's guide to cyclic voltammetry. *J. Chem. Educ.* **2017,** *95* (2), 197-206.

41. Harnisch, F.; Freguia, S., A basic tutorial on cyclic voltammetry for the investigation of electroactive microbial biofilms. *Chem. Asian J.* **2012,** *7* (3), 466-475.

42. Kissinger, P. T.; Heineman, W. R., Cyclic voltammetry. *J. Chem. Educ.* **1983,** *60*(9), 702-706.

43. Andrade, C.; Oliveira, M. D.; Faulin, T.; Hering, V.; Abdalla, D. S. P., Biosensors for detection of Low-Density Lipoprotein and its modified forms. In *Biosensors for Health, Environment and Biosecurity*, IntechOpen: Rijeka, **2011**, 215-240.

44. Scott, K., Electrochemical principles and characterization of bioelectrochemical systems. In *Microbial electrochemical and fuel Cells*, Scott, K.; Yu, E. H., Eds. Woodhead Publishing: Boston, **2016**, 29-66.

45. Fleischmann, M.; Lasserre, F.; Robinson, J.; Swan, D., The application of microelectrodes to the study of homogeneous processes coupled to electrode reactions: Part I. EC′ and CE reactions. *J. Electroanal. Chem.* **1984,** *177* (1-2), 97-114.

46. Elhadi, M. Y.; Jeffrey, K. B., Chapter 13 - Controlled Atmosphere Storage in *Postharvest Technology of Perishable Horticultural Commodities*, Woodhead Publishing: Duxford, **2019**, 439-479.

47. Gas chromatography- definition, principle, working, uses. *Online Microbiology Notes* [Online]; Sagar Aryal posted October 22, **2018** https://microbenotes.com/gas-chromatography/ (accessed Mar 10, 2020).

48. Harry, B.; Oman, Z. Trace measurement of CO, CH$_4$, and CO$_2$ in high purity gases by GC-FID-METHANIZER: method validation and uncertainty estimation. *St. Cerc. St. CICBIA*. **2017,** *18*, 259-274.

49. Mashazi, P.; Togo, C.; Limson, J.; Nyokong, T., Applications of polymerized metal tetra-amino phthalocyanines towards hydrogen peroxide detection. *J. Porphyr. Phthalocya.* **2010,** *14*, 252-263.

50. Hassel, A. W.; Fushimi, K.; Seo, M. An agar-based silver| silver chloride reference electrode for use in micro-electrochemistry. *Electrochem. Commun.,* **1999**, *1*, 180-183.

51. Smith, T. J.; Stevenson, K. J., 4 - Reference Electrodes. In *Handbook of Electrochemistry*, Zoski, C. G., Ed. Elsevier: Amsterdam, **2007**, 73-110.

52. Jawad, A.; Nathan, W. L., pH-Mediated fluorescence and G-quadruplex binding of amido phthalocyanines. *Biochemistry*. **2010**, *49*, 4339-4348.

53. Huawen L,; Thomas, F. G. Formation of electronically conductive thin films of metal phthalocyanines *via* electropolymerization. *J. Chem. Soc, Chem. Commun.,* **1989**, 832-834.

54. Joe; O.; Nazaré, P. R.; Fethi, B.; Tebello, N., Synthesis, spectral and electrochemical properties of a new family of pyrrole substituted cobalt, iron, manganese, nickel and zinc phthalocyanine complexes. *J. Porphyr. Phthalocyanines.,* **2003**, *7*, 508-520.

55. Clack, D.; Hush, N.; Woolsey, I., Reduction potentials of some metal phthalocyanines. *Inorg. Chim. Acta.,* **1976,** *19*, 129-132.

VITA

NAME Teedhat Trisukhon (Zugus)

DATE OF BIRTH 5th May 1998

PLACE OF BIRTH Angthong

INSTITUTIONS ATTENDED Chulalongkorn University

ADDRESS 42 Thetsaban 12 Rd., Tumbon Bangkaew, Ampher Mueang, Angthong 14000